



# INTERNAL CHARGE REDISTRIBUTION AND CURRENTS IN CANCEROUS LESIONS

Andras Szasz<sup>1</sup>, Gyula Vincze<sup>1</sup>, Gyula Szigeti<sup>2</sup>, Oliver Szasz<sup>1</sup>

<sup>1</sup>St. Istvan University, Dept. Biotechnics, Hungary

biotech@gek.szie.hu

<sup>2</sup>Institute of Human Physiology and Clinical Experimental Research, Semmelweis University, Hungary

## ABSTRACT

The tissues in biological objects from the point of view of electromagnetic effects have to be modeled by not only their conductivity. The electric field induced double ionic layer, constructed by electrolytic diffusion, has to be counted. We describe this phenomenon by micro (frequency dispersion phenomena), and by macro (interfacial polarization), as well as more generalized by Nernst-Planck cells. The results are applied to cancerous tissues in the healthy neighborhood. Our objective is to show the space charge distribution and redistribution that generate injury currents and other internal currents in the development of cancer. We show some aspects of the theoretical basis of modulated electro-hyperthermia (mEHT, trade name oncothermia, also used name: nanothermia), which uses an anti-injury current in the micro-range to limit the proliferation process, similar to the macro-range electrochemotherapy (ECT) processes.

## Indexing terms/Keywords

injury current, cancer wound, anti-injury current, Nernst-Planck equation, double layers, healing, regeneration, charge distribution, imperfect dielectrics, heterogeneity

## Academic Discipline And Sub-Disciplines

Biology

## SUBJECT CLASSIFICATION

Biophysics

## TYPE (METHOD/APPROACH)

Theoretical considerations

## INTRODUCTION

To understand the basic electromagnetic interactions is a crucial demand generally in biophysics, and especially in active treatments, like hyperthermia or other electromagnetic modes of therapies; and passive adaptations, like bioelectromagnetic diagnostics, as well as the very popular “electrosmog”. Understanding the main effects is definitely a major point in many applications besides expecting explanations on the basic technical differences of the nowadays widely applied oncological hyperthermia treatments as well.

### General considerations

Two parameters are used to characterize tissues from an electric point of view: the conductivity and the dielectric permittivity. We know, however, that tissue at low frequencies can be modeled only with isolated spheres (cells) and conductive, multicomponent electrolytes around them (extracellular liquid). Consequently, in this system, the conduction is ionic, which is trivially accompanied by chemical mass-transport.

Charge conservation (continuity equation) requires the normal component of the total current density to be continuous at the phase boundaries. Due to the chemical and ionic concentration and dielectric differences, as well as the various diffusion and mobility constants of the relevant tissues, charges, and chemical components can change on the phase boundary.

In a former model, the unity cube of the tissue could be electronically substituted by the expletive schematics; (see Figure 1).

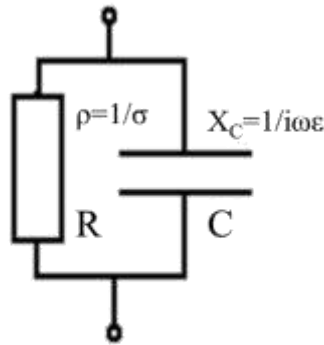


**Fig 1: Expletive electronic circuit R,C, Xc is the reactance (high-frequency resistance) of the capacitor, ρ is the specific resistivity of the resistor. Ω is the actual circular frequency (ω=2πf, where f is the frequency of the supply).**

We show how the concept based on this picture misleads. The basic contradictory point is that the electrodes of the condenser can have extra charges, which is not the case in the real biological matter (i.e. tissue).

The question is: can the phase boundaries between various tissues be introduced only by the real tissue interfaces or by the electrode-tissue interfaces? The last boundary is evident from the fact that the electrode has electronic conductivity only, while the skin (and the subsequent tissues) has mainly ionic conduction. This means that there is an interface converting the electronic conduction to the ionic one. This phenomenon is similar to the other electrode processes, e.g. platinum electrodes, lead-sulphate/oxide for batteries, etc.

If we would like to construct a more realistic expletive schematic, then we have to consider the double layer on the electrode surfaces, where the metal is negatively, and the electrolyte in contact will be positively charged.

### Induced space-charge forming in heterogeneous dielectrics

This phenomenon is characteristic of heterogeneous dielectric materials, cell-membranes, like tissues and organs.

The Gauss law and the charge conservation with E field vector, ρ charge density, σ conductivity and J electric current is:

$$\text{div}\underline{E} = \rho, \quad \underline{J} = \sigma\underline{E}, \quad \frac{\partial \rho}{\partial t} + \text{div}\underline{J} = 0 \quad (1)$$

Consequently in harmonic fields by ω circular frequency ( $i = \sqrt{-1}$ ):

$$\text{div}(i\omega\varepsilon + \sigma)\underline{E} = 0 \quad (2)$$

Hence:

$$\begin{aligned} \text{grad}\varepsilon \cdot \underline{E} + \varepsilon \text{div}\underline{E} &= \rho & (3) \\ \text{grad}\sigma^* \cdot \underline{E} + \sigma^* \text{div}\underline{E} &= 0, \\ \sigma^* &= (i\omega\varepsilon + \sigma) \end{aligned}$$

Further simplification:

$$[\text{grad}\varepsilon + \text{grad}(\ln \sigma^*)]\underline{E} = \rho \quad (4)$$

The gradient of permittivity determines the behavior, which linearly depends on the E field. The logarithm of the conductivity smooths its changes, so it has a minor effect on the charge. The effect is frequency-dependent (i.e. both ε and σ change), but no structural components are involved.

### Macroscopic effects on tissue heterogeneities (interfacial polarization)

Inhomogeneous dielectric material (like living tissues, and their higher organizations) creates space charge due to the permittivity gradient, according to (4). The accumulated space charge increases the charge of the capacitor, consequently the value of the capacity as well, when the structure does not change. The space-charge is also frequency-dependent (like the microscopic membrane effect) because the conductivity (and due to this the permittivity too) is frequency-dependent.

The simplest arrangement to show interfacial polarization is a condenser with two layers of permittivity between its electrodes. The space charge will be created at the boundaries of the permittivity blocks, which are parallel to the

electrodes. We study first a homogeneous dielectric material with parameters  $\epsilon$ ,  $\sigma$  and  $d$  thickness creating  $U$  potential with the  $E$ -field by  $I$  current, with the unit area ( $A$ ) of the electrode as in (Figure 2).

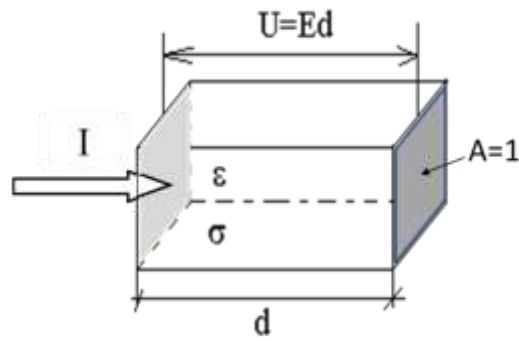


**Fig 2: Homogeneous dielectric block**

The current (due to the unity of the electrode surface) in equal value to the current density ( $J$ ) will be:

$$I = J = \frac{\partial D}{\partial t} + J_{cond} = (i\omega\epsilon + \sigma)E = \sigma^* \frac{U}{d}, \quad (5)$$

$$\sigma^* = i\omega\epsilon + \sigma = i\omega \left( \epsilon - i \frac{\sigma}{\omega} \right) = i\omega(\epsilon' - i\epsilon''),$$

$$\epsilon' := \epsilon \quad \epsilon'' := \frac{\sigma}{\omega}$$

where the complex conductivity ( $\sigma^*$ ) and complex permittivity ( $\epsilon^* = \epsilon' + i\epsilon''$ ) are introduced. Analogy introduces average impedance and conductivity to Ohm's Law:

$$Z := \frac{U}{I} = \frac{d}{\sigma^*}, \quad Y := \frac{I}{U} = \frac{\sigma^*}{d} \quad (6)$$

When two different dielectric materials with  $d_1$  and  $d_2$  thickness with the same unit area are in a serial arrangement in the condenser (Figure 3), then:

$$Z = \frac{d_1}{\sigma_1^*} + \frac{d_2}{\sigma_2^*} \quad (7)$$

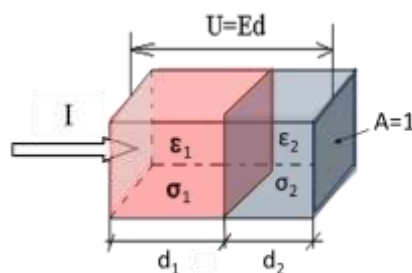


**Fig 3: Arrangement of two dielectric materials in the condenser**

We define the conductivity of this composite dielectric block by:

$$\frac{d_1 + d_2}{\sigma^*} = Z = \frac{d_1}{\sigma_1^*} + \frac{d_2}{\sigma_2^*} \quad (8)$$

From this definition, we receive the independent geometry conductivity and complex permittivity depending only on the ratio of volumes:



$$\sigma^* = \frac{\sigma_1^* \sigma_2^*}{a(\sigma_2^* - \sigma_1^*) + \sigma_1^*}, \quad (9)$$

$$\varepsilon^* = \frac{\sigma^*}{j\omega} = \frac{\sigma_1^* \sigma_2^*}{j\omega [a(\sigma_2^* - \sigma_1^*) + \sigma_1^*]}$$

$$a = \frac{d_1}{d_1 + d_2}$$

A parameter represents the geometry, showing that the complete solution is solely dependent on the layer thickness. The parallel blocks are irrelevant, because the gradient and the field are perpendiculars, and their scalar product is zero. Hence we obtain:

$$\varepsilon^* = \varepsilon_\infty + \frac{\varepsilon_s - \varepsilon_\infty}{1 + j\omega\tau} + \frac{\sigma_s}{j\omega} \quad (10)$$

$$\varepsilon_\infty = \frac{\varepsilon_1 \varepsilon_2}{a(\varepsilon_2 - \varepsilon_1) + \varepsilon_1},$$

$$\varepsilon_s = \frac{(\sigma_1 \varepsilon_2 - \sigma_2 \varepsilon_1)^2 a(1-a)}{[a(\varepsilon_2 - \varepsilon_1) + \varepsilon_1][a(\sigma_2 - \sigma_1) + \sigma_1]^2} + \varepsilon_\infty,$$

$$\tau = \frac{a(\varepsilon_2 - \varepsilon_1) + \varepsilon_1}{a(\sigma_2 - \sigma_1) + \sigma_1},$$

$$\sigma_s = \frac{\sigma_1 \sigma_2}{a(\sigma_2 - \sigma_1) + \sigma_1}$$

This result is remarkable: the inhomogeneous dielectric arrangement could have larger dielectric permittivity than the individual components. The permittivity, in this case, is a complex value, which is frequency-dependent and can be approximated by the Debye principles.

The biological material is imperfect dielectrics, having displacement current and conductive current as well. The conduction is mainly ionic in an aqueous electrolyte, in the body fluids.

The current density of the bio-matter is:

$$j_{tot} = \frac{\partial D}{\partial t} + j_{cond} \quad (11)$$

where  $D = \varepsilon E$ , and  $j_{tot}$  the complete,  $j_{cond}$  the conductive part of the current density. The current densities depend linearly on the small electric fields. Consequently, the Fourier transform of the total current density, in this case, is similar to the simple differential version of Ohm's Law:

$$j_{tot}(j\omega) = [i\omega\varepsilon(j\omega) + \sigma_s]E(j\omega) \quad (12)$$

Following this analogy, the complex conductivity is:

$$j_{tot}(i\omega) = [i\omega\varepsilon(i\omega) + \sigma_s]E(i\omega) = \sigma^* E(i\omega), \quad (13)$$

$$\sigma^* := i\omega\varepsilon(i\omega) + \sigma_s$$

The first term of  $\sigma^*$  is the capacitive conductivity, while the second is ohmic. This equation could be formally written in the same form as in the ideal dielectric material, which is in sinusoidal fields:

$$\frac{\partial D}{\partial t} = \varepsilon \frac{\partial E}{\partial t} \rightarrow \frac{\partial D}{\partial t} = i\omega\varepsilon E \quad (14)$$

and:



$$j_{tot}(i\omega) = i\omega \left[ \varepsilon(i\omega) + \frac{\sigma_s}{i\omega} \right] E(i\omega) := i\omega \varepsilon^*(i\omega) E(i\omega), \quad (15)$$

$$\varepsilon^*(i\omega) = \varepsilon(i\omega) + \frac{\sigma_s}{i\omega} = \varepsilon(i\omega) - i \frac{\sigma_s}{\omega} := \varepsilon' - i\varepsilon''$$

where  $\varepsilon^*(j\omega)$  is the complex dielectric permittivity, where:

$$\varepsilon' := \varepsilon(i\omega), \quad (16)$$

$$\varepsilon'' := \frac{\sigma_s}{\omega}$$

Consequently:

$$\sigma^* = i\omega \varepsilon^* \quad (17)$$

The dielectric permittivity depends on the frequency, causing dispersion. The simple theory of dispersion was laid out by Debye [1]. The complex dielectric material in this description has three parameters: the permittivity at high frequencies ( $\varepsilon_\infty$ ), the permittivity at low frequencies ( $\varepsilon_s$ ), and the breaking-point circular frequency ( $\omega_0 = 2\pi f_0$ ), characterizing the transition between the two states. According to Debye:

$$\varepsilon(i\omega) = \varepsilon_\infty + \frac{\varepsilon_s - \varepsilon_\infty}{1 + i \frac{\omega}{\omega_0}} \quad (18)$$

The relaxation time is the reciprocal value of  $\omega_0$ .

$$\varepsilon(i\omega) = \varepsilon_\infty + \frac{\varepsilon_s - \varepsilon_\infty}{1 + i\omega\tau}, \quad (19)$$

$$\tau = 1/\omega_0$$

The physical meaning of this relaxation time is the time during the displacement vector oriented by the switched-on unit electric field.

When their frequency is at the breaking point ( $\omega = \omega_0$ ), then:

$$\varepsilon(i\omega_0) - \varepsilon_\infty = \frac{\varepsilon_s - \varepsilon_\infty}{1 + i \frac{\omega_0}{\omega_0}} = \frac{\varepsilon_s - \varepsilon_\infty}{1 + i} \rightarrow \quad (20)$$

$$|\varepsilon(i\omega_0) - \varepsilon_\infty| = \frac{\varepsilon_s - \varepsilon_\infty}{\sqrt{2}} \rightarrow \frac{|\varepsilon(i\omega_0) - \varepsilon_\infty|}{\varepsilon_s - \varepsilon_\infty} = \frac{1}{\sqrt{2}}$$

So the complex permittivity of the bio-matter is:

$$\varepsilon^*(i\omega) = \varepsilon_\infty + \frac{\varepsilon_s - \varepsilon_\infty}{1 + i\omega\tau} + \frac{\sigma_s}{i\omega} \quad (21)$$

Hence the relative permittivity:

$$\varepsilon_r^*(i\omega) = \varepsilon_{r\infty} + \frac{\varepsilon_{rs} - \varepsilon_{r\infty}}{1 + i\omega\tau} + \frac{\sigma_s}{i\omega\varepsilon_0} \quad (22)$$

where the subscript r denotes the relative value, while  $\varepsilon_0$  is the permittivity of a vacuum. The electric circuit that models (22) is shown in (Figure 4).

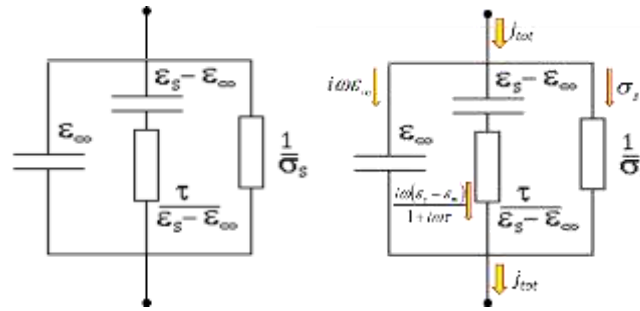


**Fig 4: This circuit represents a unit-edge cube from the bio matter; the impedance is measured between two parallel sides. The currents are divided by the parts of complex resistivity**

The product of the permittivity and the value of  $\frac{\tau}{\epsilon_s - \epsilon_\infty}$  as specific resistivity is the time-constant (see (10)). The numerical value is equal to the current density, which is induced by unit electric field according to (13). From this, the current densities (shown in Fig 4) are:

$$i\omega\epsilon_\infty, \quad (23)$$

$$\sigma_s,$$

$$\frac{1}{\frac{1}{i\omega(\epsilon_s - \epsilon_\infty)} + \frac{\tau}{\epsilon_s - \epsilon_\infty}} = \frac{i\omega(\epsilon_s - \epsilon_\infty)}{1 + i\omega\tau}$$

Hence (using (17) the total current density and the complex conductivity are

$$\sigma^*(i\omega) = i\omega \left[ \epsilon_\infty + \frac{\epsilon_s - \epsilon_\infty}{1 + i\omega\tau} + \frac{\sigma_s}{i\omega} \right] = i\omega\epsilon^*(i\omega), \quad (24)$$

$$\epsilon^*(i\omega) = \epsilon_\infty + \frac{\epsilon_s - \epsilon_\infty}{1 + i\omega\tau} + \frac{\sigma_s}{i\omega}$$

Consequently, the real and imaginary permittivity are:

$$\epsilon' = \epsilon_\infty + \frac{\epsilon_s - \epsilon_\infty}{1 + (\omega\tau)^2} \quad (25)$$

$$\epsilon'' = \frac{\sigma_s}{\omega\epsilon_0} + \frac{\omega\tau(\epsilon_s - \epsilon_\infty)}{1 + (\omega\tau)^2},$$

$$\epsilon' = \text{Re}(\epsilon^*)$$

$$\epsilon'' = -\text{Im}(\epsilon^*)$$

The energy absorption components in the volume unit are:

$$s = \frac{1}{2} E \hat{j} = \frac{1}{2} \hat{\sigma}^* E \hat{E} = -\frac{1}{2} j\omega \hat{\epsilon}^* E^2 = -\frac{1}{2} \omega (j\epsilon' + \epsilon'') E^2 \quad (26)$$

$$w = \text{Im}(s) = -\frac{1}{2} \omega \epsilon' E^2$$

$$p = \text{Re}(s) = \frac{1}{2} \text{Re}(E \hat{j}^{(*)}) = \frac{1}{2} \omega \epsilon'' E^2$$

where  $s$  is the apparent absorption,  $w$  is the reactive absorption, which periodically goes in and out of the system by double frequency, and  $p$  is the real Joule heat.

#### Microscopic effects on membranes ( $\beta/\delta$ -dispersion)

The radio-frequency (RF) current does not flow through the tissue homogeneously when the frequency does not exceed 15 MHz; see Figure 5.

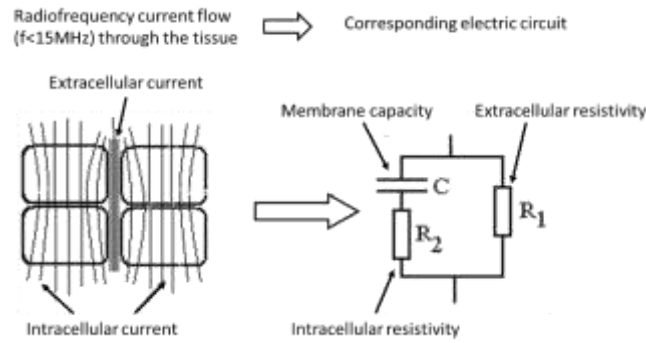


**Fig 5. The current flow selects between the extracellular and intracellular electrolytes in the range of radiofrequency <math>< 15\text{MHz}</math>, and could be modelled by the shown electric circuit.**

The consequent conductivity is:

$$\sigma_{\Sigma} = \frac{1}{R_1} + \frac{1}{\frac{1}{i\omega C} + R_2} \quad (27)$$

It is frequency-dependent. Its slope of change of  $\sigma$  is large, at around  $f=10\text{ MHz}$ , at the range of  $\beta/\delta$ -dispersion, [2,3], consequently the accumulation of charges here are the largest; (see Figure 6).

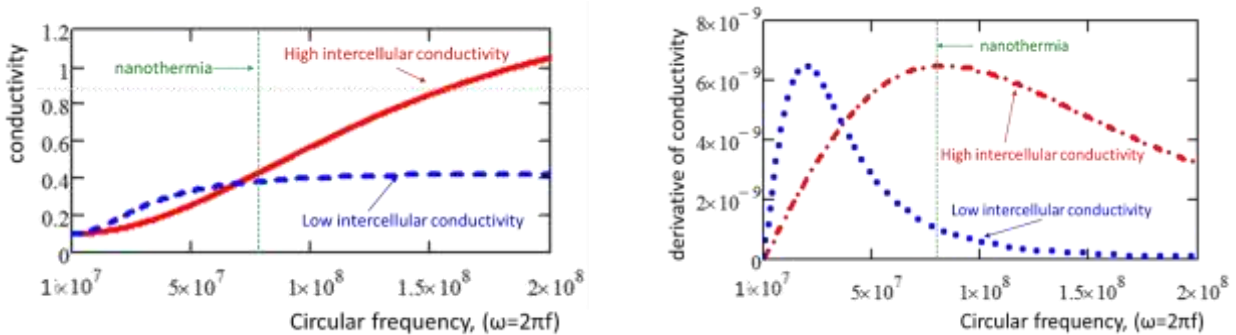


**Fig 6: The conductivity (a) and its derivative(b) at high ( $R_2=3$ ) and low ( $R_2=0.7$ ) resistivity (low ( $1/3$ ) and high ( $1/0.7$ ) conductivity) of cytoplasm ( $C=10^{-8}$ ;  $R_1=10$ ,  $\omega = 8.522 \times 10^7$  1/s [ $f=13.56\text{ MHz}$ ])**

Beta dispersion is the phenomenon associated with the ability of a biological cell membrane to filter out low-frequency currents and allow high-frequency currents to pass through [4].

The main reason for the  $\beta$ -dispersion is the higher penetration of the RF-current into the intracellular electrolyte by the increasing frequency. With this effect, the capacitive conduction of the membrane grows. The place of  $\beta$ -dispersion has a high derivative and the gradient of permittivity is higher; consequently the accumulated charge is higher. Additional growth of permittivity of the membrane takes place by the  $\delta$ -dispersion [5], in the same range as the maximum of the derivative, around 10–14 MHz, which increases further the charge separation. Note that when the gradients of permittivity and conductivity are perpendicular on the penetrated external field, space-charge is not formed.

### Nernst-Planck formulation of space-charge

The Nernst-Planck type space charge [6] can be formed in every non-perfect dielectric material, e.g. biological objects. It could be applied even in porous media. [7].

Local hyperthermia by electromagnetic interactions is extensively used in oncology. Various technical solutions exist, where the electric field develops the real heat. The specific absorption rate (SAR) determines the heating ability [8].

The technical solution when the electric field acts simply is capacitive coupling. The capacitive coupling in oncological hyperthermia was established in the middle of the 1970s [9], and has been a widely applied method until the present [10]. The applied field is controllable, and the technique is applicable for all of the tumour-lesions. Due to the technically well-controlled external electric field from the parallel electrodes of capacitive coupling, we use in the calculations the E-field only. The heating is the stationary case from bio-heat equation is:

$$c_b(T - T_b) = \frac{1}{2} \sigma |E|^2 = SAR \quad (28)$$

where  $c_b$  is the blood perfusion rate,  $T_b$  is the blood temperature.

The tissue boundaries are inhomogeneous interfaces, where extra field strengths ( $E(i)$ ) could be generated. Ohm's Law is in this case:

$$\underline{j} = \sigma(\underline{E} + \underline{E}^{(i)}) \quad (29)$$

In the following we use an electric field, which is directed to the x-axis of the space, so we will not denote the vectors. The charge continuity equation is:

$$\frac{\partial \rho}{\partial t} = -\frac{\sigma}{\epsilon} \rho - \sigma \frac{\partial E^{(i)}}{\partial x} = -\frac{\sigma}{\epsilon} (\rho - \rho^{(i)}) \quad (30)$$

$$\rho^{(i)} = \epsilon \frac{\partial E^{(i)}}{\partial x}$$

Its solution is:

$$\rho = \rho^{(i)} + \rho_0 e^{-\frac{t}{\tau}} \quad (31)$$

Consequently, the perturbation exponentially decays, but space charge remains due to the inhomogeneity. The time constant differs from the previous one, and it is the same order of magnitude as the periodic time.

We show next that in this case, the parallel R-C circuit is a correct expletive schematic and the condenser electrode is the phase boundary. The expletive schematics (Figure 7), show two connected layers indicating the interface (transition layer) between them.

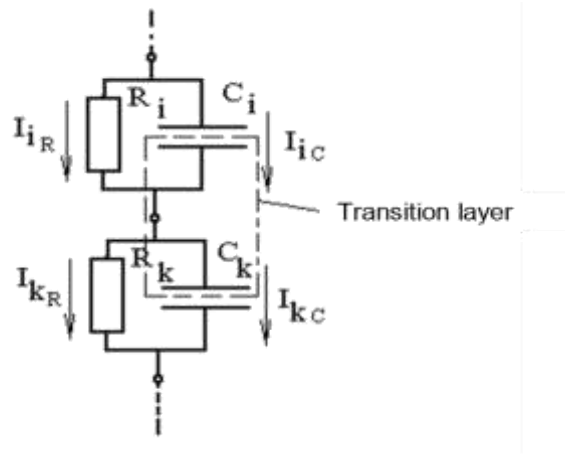


**Fig 7: Expletive schematics for interfaces in serial connection**

The charge of the condensers in the interface is:

$$Q_i = -C_i U_i = -C_i R_i I_{iR} = -\tau_i I_{iR} \quad (32)$$

$$Q_k = C_k U_k = C_k R_k I_{kR} = \tau_k I_{kR}$$

Moreover, the resultant surface charge:

$$q = \frac{Q_k + Q_i}{A} = \tau_k j_{kR} - \tau_i j_{iR} \quad (33)$$

where A is the surface of the electrodes (i.e. the plate condenser).

Due to the possible variance of time constants and surface currents, surface free charge exists. Consequently, we have to use the other model, because this is applicable only in the case of charge accumulation in the transition layer. Its condition is the commensurable time constant with the quarter of the periodic time. The schematic of the corrected model is shown in (Figure 8). We consider the electric conduction and the diffusion- and drift-like material transport as well. This new model has Nernst-Plank characteristics, so we refer to it as a Nernst-Plank cell.

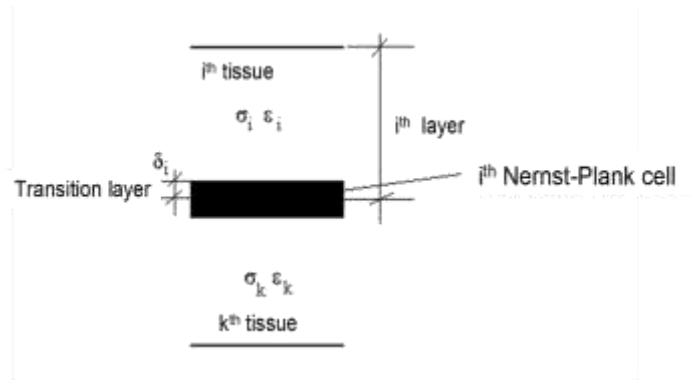


**Fig 8: Schematic of the corrected model**

The current density versus field strength connection (i.e. the characteristics of the Nernst-Plank cell) could be described by the generalized Ohm's Law for inhomogeneous media. In real cases, various chemical species are transported through tissue. The charge transport is connected to the mass transfer, which could be described by the generalized current densities. Principally, it has two current density components: the drift forced by field strength and the diffusion current driven by the concentration gradients. We calculate these for one chemical component using a linear approach.

We take the concentration  $C(x)$  of the chemical component at  $x$ , so, according to Fick's Law, the diffusive current density is:

$$j_{id} = -D \frac{dC(x)}{dx} \quad (34)$$

where  $D$  is the diffusion constant of the given chemical component. We denote the ionizing level of the given chemical component by  $Z$ , and its ion mobility by  $\beta$ . Then at the applied  $E$  field-strength, the drift velocity is:

$$v_{drift} = -\beta E \quad (35)$$

which (using the Einstein relation) could also be written in the form:

$$v_{drift} = -\beta e E = -\frac{kT}{D} e E \quad (36)$$

where  $e$  is the elementary charge (electron charge),  $k$  is the Boltzmann constant, and  $T$  is the tissue temperature. Hence, the drift-current density in the transition layer is:

$$j_{drift} = -C(x) \frac{kT}{D} Z e E \quad (37)$$

Therefore, the particle current density of the chemical component is:

$$j = -D \frac{dC(x)}{dx} - C(x) \frac{kT}{D} Z e E \quad (38)$$

From this the jointly transported electric current density is:

$$j_e = Z e j = -Z e D \frac{dC(x)}{dx} - C(x) \frac{kT}{D} Z^2 e^2 E \quad (39)$$

which looks in Ohm's Law-form like:

$$\begin{aligned} j_e &= \sigma (E + E^{(i)}), \\ \sigma &= C_0(x) \frac{kT}{D} Z^2 e^2 \\ E^{(i)} &= -\frac{Z e D}{\sigma} \frac{dC(x)}{dx} \end{aligned} \quad (40)$$

For numerical investigation we normalize these values:

$$j := \frac{j_e}{\frac{ZeDC_2}{\delta}} = \frac{\frac{C_1}{C_2} e^{-\frac{ZeU}{kT}} - 1}{e^{-\frac{ZeU}{kT}} - 1} \frac{ZeU}{kT} = \frac{xe^{-u} - 1}{e^{-u} - 1} u, \quad (41)$$

$$u = \frac{ZeU}{kT}, \quad x := \frac{C_1}{C_2}$$

This result shows that the “foreign” field strength appears only where the particle concentration has a gradient (e.g. in the phase boundaries).

Suppose a linear change of the potential in the transient layer; the equations above can now be solved easily:

$$j_e = \frac{Z^2 e^2 D}{kT\delta} \frac{C_1 e^{-\frac{ZeU}{kT}} - C_2}{e^{-\frac{ZeU}{kT}} - 1} U \quad (42)$$

where  $C_1$  and  $C_2$  are the concentrations of the interface layer incident and emergent sides, and  $\delta$  is the thickness of the transition layer by U potential-drop on it. Analyzing this result, we have the following approximations:

1. If  $|U|$  is a small value then from (42):

$$j_e = \frac{Z^2 e^2 DC_1}{kT\delta} U \quad (43)$$

so, the simple form of Ohm’s Law is valid in this case also.

2. If U is a large positive potential, then from (42):

$$j_e = \frac{Z^2 e^2 DC_2}{kT\delta} U \quad (44)$$

Ohm’s Law is valid with  $\sigma_2 = \frac{Z^2 e^2 DC_2}{kT\delta}$  conductivity;

3. If U is a large negative potential, then from (42):

$$j_e = \frac{Z^2 e^2 DC_1}{kT\delta} U \quad (45)$$

Ohm’s Law is valid with  $\sigma_1 = \frac{Z^2 e^2 DC_1}{kT\delta}$  conductivity.

The two conductivity values are different due to the concentration variance.

As a result of this, the Nernst-Plank cell is a potential dependent two-pole with nonlinear characteristics, as its conductivity depends on the direction of the current. Hence, the cell rectifies and distorts, so, for example, the supplied sinusoidal potential will gain a non-sinusoidal current containing upper harmonics. This result is numerically shown by calculation (Figure 9).

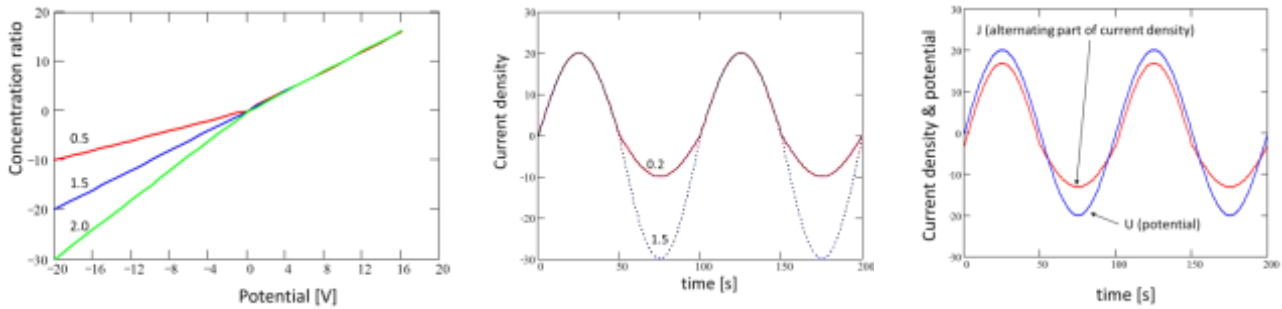


**Fig 9. Nernst-Plank cell characteristics with various concentration ratios of  $x=0.5, 1.0, 1.5$ . (a); Comparison of current densities vs. time for two different cells (concentration ratios: 0.2, and 1.5) (b); Comparison of the potential and the current density. (at a concentration ratio of 0.21) (c)**

On this basis, the correctness of this model is easy to prove: if we have over harmonics on a harmonic potential excitation, then we have the Nernst-Plank cell as well.

One quarter of the wavelength of the used 13.56 MHz potential supply is larger than the geometric size of the treated region. This is a near-field application; therefore no radiative wave phenomenon could be included (for the waves, both the

magnetic and electric displacements currents are essential. In our case, the magnetic displacement current  $\frac{\partial \bar{B}}{\partial t}$  is negligible).

At these conditions:

$$\text{rot} \underline{E} = 0 \rightarrow \underline{E} = -\text{grad} U \quad (46)$$

moreover, on the other hand from Maxwell's Third Equation:

$$\text{rot} \underline{H} = \underline{j} + \frac{\partial \underline{D}}{\partial t} = \underline{j}_e + i\omega \epsilon \underline{E} \rightarrow \text{div} \text{rot} \underline{H} = \text{div}(\underline{j}_e + i\omega \epsilon \underline{E}) = 0 \quad (47)$$

In the former model (Fig. 1), Ohm's Law is:

$$\bar{j}_e = \sigma \bar{E} \quad (48)$$

The field is therefore determined by the Laplace Equation:

$$\text{div}(\sigma + i\omega \epsilon) \underline{E} = \text{div}(\sigma + i\omega \epsilon)(-\text{grad} U) = 0 \quad (49)$$

In the realistic model, Ohm's Law is:

$$\underline{j}_e = \sigma(\underline{E} + \underline{E}^{(i)}) \quad (50)$$

For what we have to use the Poisson Equation:

$$\text{div}(\sigma + i\omega \epsilon) \underline{E} + \text{div}(\sigma \underline{E}^{(i)}) = 0 \rightarrow \text{div}(\sigma + i\omega \epsilon)(\text{grad} U) = \text{div}(\sigma \underline{E}^{(i)}) \quad (51)$$

The two Poisson Equations have considerable differences on the phase boundaries. Consequently, the results for the local heating are different to the two approaches. The phantoms used for the models of heating have no phase boundaries, so the calculation is incorrect and cannot be used for indication by the treatments.

The apparent phase shift observation is also misleading. No phase shift exists. We show it by harmonic analysis. The frequency spectrum of the current density is shown in (Figure 10).

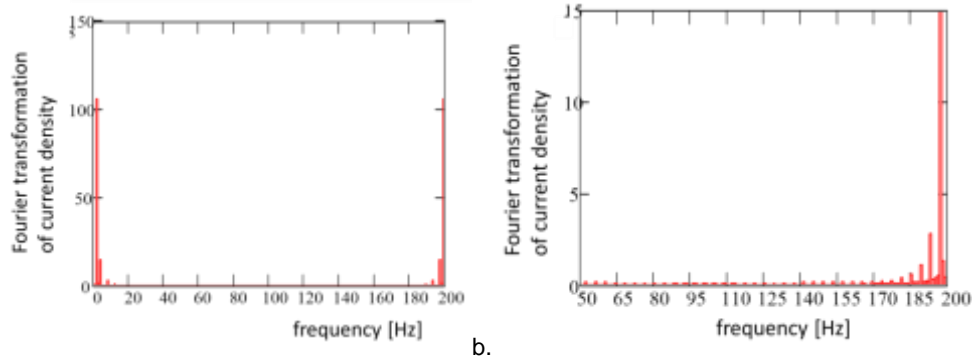


**Fig 10: Frequency spectrum by Fourier transformation of the alternating part of the current density (at concentration ratio 0.21) (a) and magnification of the upper harmonic range (b)**

The spectrum is obviously limited by frequencies and contains high peaks (Figure 10b). The time function magnification of the upper harmonic range and the basic current harmonics with the potential are shown in (Figure 11).

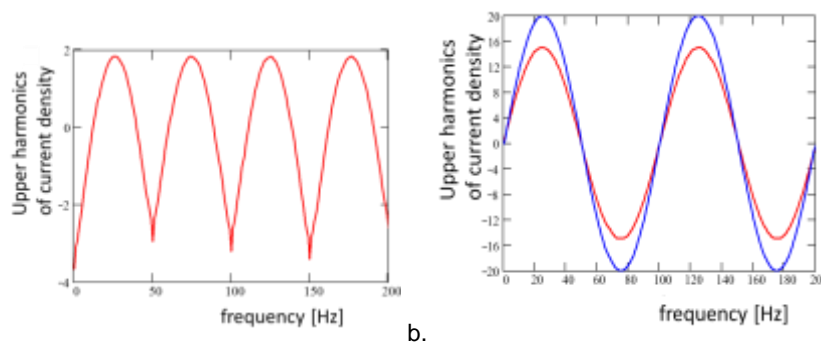


**Fig 11: Time function of the upper harmonics of the current density (a) and the basic harmonic of current and the potential in time (b) (at concentration ratio = 0.21).**

The time function of the basic harmonics of potential and current density and the frequency spectrum of the residual current density are shown in (Figure 12).

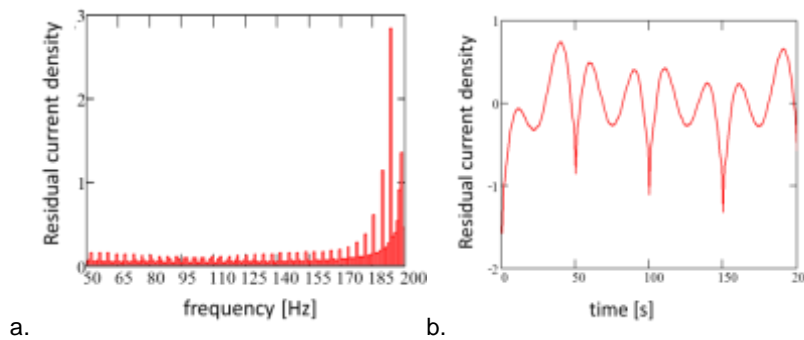


**Fig 12: Frequency spectrum of the residual current density (a) and time function of the residual current density (b), (at concentration ratio = 0.21).**

The comparison of the time function of the first upper harmonic potential and current amplitudes for concentration ratios  $x=0.21$  and  $x=2.091$  are shown in (Figure 13).

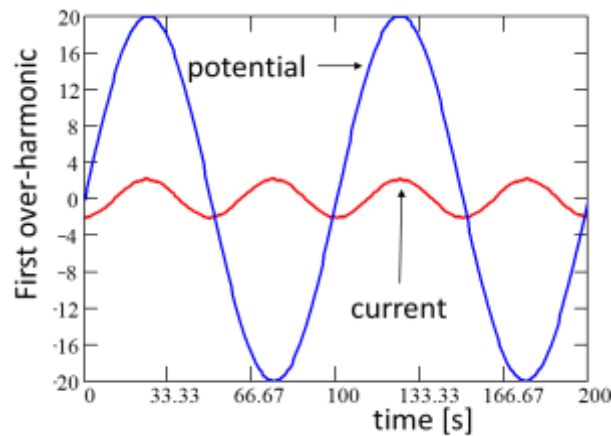


**Fig 13: Time function of the first upper harmonic potential and current amplitude (at concentration ratio = 2.091).**

### Space charge without external inducing

Cells, tissues, and organs have internal polarization, which is a crucial factor of the interactions in the living system [11]. All cells have various membranes defining the fundamental functions of the cells. All membrane structures are strictly polarized layers, separating the various electrolytes and governing the selective ionic exchanges. Well-known polarization characterizes many tissues, like epithelial separating adjacent tissues from each other and having a specific role in the homeostasis of organs. Epithelia form a well-structured layer; it is a permanently polarized sheet fixing the post-developed complete organism for its entire life. The human body has definite polarization measured on the skin in the whole body surface [12].

The polarization is fundamental not only in epithelial cells but active in many tissues in the organisms. It arranges the water structure to polarize too, which shows semi-crystalline behavior in this way [13]. It is likely that the ordered water bound to the membrane is oriented by the membrane potential, and by the polarized epithelial sheets as well.

Polarization is a charge separation and represents an enormous electric field by their static arrangement. For example, a 7 nm-thick cell membrane that has 70 mV membrane potential represents an electric field of 10 million V/m, which is an enormous value. This field is fixed in a condenser-like construction. It is stable: no extra charge flow is generated by this high electric field in normal functions of the body. However, any injury may produce a potential difference between the parts of the tissue, which induces electric currents (constrained ion-flow) in the tissue, without being triggered by an external electric field.

The physical meaning of polarization is the formation of the double layer with charges in heterogenic media. Internally and also with the external field, the non-perfect dielectric materials have an internal field addition due to the polarization. When the polarization is internal (i.e. no external field triggers), it is in the stationary state, is stable, and does not induce any current. However, when the integrity of living tissue is perturbed, injury of other disturbances rearranges the actual state, and current is generated due to the potential difference in the conductive media. In the case of an injury, the wound in the epithelium provides a short-cut: its potential tends to zero in this localization. However, at a distance of 0.5–1 mm, the original potential value can be measured, causing a certain gradient of the electric field. This difference of electric field induces an electric current directed to the wound. The current, powered by this process of the endogenous field-strength, is called the injury current [14].

The injury current certainly plays a central role in wound healing [15]. Injury currents are physiological [16], and their typical value is around 100  $\mu\text{A}/\text{cm}^2$  on the physiological potential gradient drops  $\sim 100$  mV/cm and may be extended to the mm distance from the wound [17]. This very weak power ( $\sim 0.01$  mW/g) does not increase the local temperature [18], but can be measured using high-tech methods during the wound-healing process [19], [20], [21]. The EF in the tissue is oriented to the wounded area. The current has an electric circuit loop through the surface of the epithelium, where the electric current travels to the surface from the depth of the wound itself. This electrically controls the wound-healing process and persists as long as the wound exists. The frequency of the cell division and space-orientation of the cells are determined by the electric field [22], and it directs the cell migration to heal the wound [23], [24]. Spontaneous biological charge transfers have significant role, being one of the basic phenomena of tissue repair [25], [26], and especially control the cells and heal the wound by electrical manipulations [27]. The injury current concept is well proven [28], [29], [30], [31]. It needs sensitive experimental setups to measure, but many invasive [32], [33], and noninvasive [34], [35], [36] measurements have been performed to prove the current experimentally.

The current flow in the presence of external fields is well known in conductors. We have shown above the polarization effect by external electric fields in imperfect conductors in macro and micro range even in "porous" conditions like the cellular structure. This polarization differs from that that induces injury current when its stability is disturbed. Contrary to the internal polarization, the external triggering has no stable (current free) state, when the external field is time-varying (i.e. alternating). In the cases of electric currents, irrespective of the internal or external sources, the conductivity and the electric field induced processes by the polarized layers constructed by electrolytic diffusion has to be counted (Figure 14). These electric current are called bio-currents.

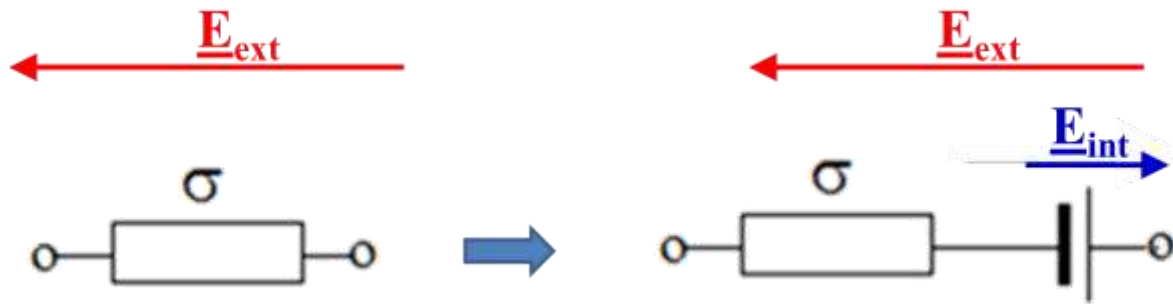


**Fig 14: Model of the effect of the Nernst-Planck principle. The non-perfect dielectric material develops an internal electric field by double layer in an external electric field. The model has an additional field substitute: the simple resistivity alone.**

While the currents caused by disturbance of internal polarization structure are directed to the place of disturbance, the current induced by polarization with external field changes its direction as the field varies. This may support the injury current and may oppose it, flowing in the opposite direction, and suppressing the expected migrations for wound healing. The reverse current is the anti-injury current.

### Cancer

These are spontaneous biological charge transfers that have an important role, which is hypothesized and are supported by some observations [37], [38]. A bioelectromagnetic hypothesis of “biologically closed electric circuits” (BCEC) was developed. BCEC introduced the existence of intrinsic electric currents in the body, mainly through the low-resistance vascular network, [39], [40] like wiring. The pathological disorders induce these currents (like a wound does). We may use this phenomenon for cancerous tissues in the healthy neighborhood. The double layer on the border of a tumor induces an electric field, which generates current to an additional extra effect to the external field application.

The malignant cells are more negative on their surface than their healthy counterparts [41], and their membrane potential is markedly lower [42], [43]. A certain potential gradient between malignant tissue and its healthy neighborhood exists [39], [44]. The gradient acts to promote and direct the cancer-cell migration [45]. There is an argument on the cancerous process as a wound repairs [46]. The bio-sy stem falsely recognizes a tumor as a wound and stimulates its environment to heal the irregularity, cure the wound. The injury currents produced by the potential gradients support the wound-healing mechanism actively. Using the BCEC principle, the anti-injury current is introduced to block the false wound healing for tumor lesion [47], [48]. This direct current is applied as therapy electrochemotherapy (ECT) of cancer. ECT is a well-established method of cancer treatment [44], [49], [50]. ECT applies a non-ablative static electric field to generate currents (using less than 5 W power). It has been found to be efficient against cancer [17], [51], [52]. Early results were amazing and were well accepted soon in Japan and China [53], [54], [55] with results reported in several peer-reviewed journals [56], [57], [58], [59], [60]. However, the method is invasive, and a non-invasive safe method was demanded.

The permittivity gradient is opposite to the field strength vector, due to the relative negative charge of cancer. To compensate for the negative space charge, the field constraints electric current to the cancer-disk, starting an injury current between the cancerous and healthy parts. This current could differentiate between the healthy cells and the multipotent ones, which became autonomic and redifferentiated to cancerous. This mechanism creates the “precancerous cells” measured by Loewenstein [61]. The challenge is that the injury current is not able to compensate for the space charge. Due to the high metabolic rate, the cancerous cells are in the permanent division and produce the negative space-charge. Therefore the natural mechanisms of the bio-system are not able to block the cancerous development after a definite size. Artificial intervention to deliver positive charges to compensate the intrinsic currents could be helpful. For this task, the necessary electric field-strength has to be a parallel vector to the gradient of the permittivity.

However, the effect of body electrolytes on the electrode surface in the chemically reactive biomaterial causes the next problem: due to the developing Warburg impedance [62]. The DC current is quickly compensated for by the double layer on the applied electrodes. The boundary between the target and the electrode affects the impedance by building up a polarized layer. There are several important phenomena of the electrodes, even if they are indifferent (i.e. the electrode does not dissolve in the electrolyte. This is the case for the well-chosen invasive electrode or the non-invasive surface touching as well).

The double layer on the border of a tumor induces an electric field, which generates current to add extra effect over the external field application. This double layer represents an electromotive force as well, which has to be included in the calculation like an electrolytic polarization under the electrodes. Its value is determined by the electrode materials and electrolyte composition; and also depends on the frequency (dispersion) and the direction of the current.

We calculate the relaxation time of the double layer construction studying the charge continuity equation in one dimension:

$$\frac{\partial \rho}{\partial t} + \frac{\partial j}{\partial x} = 0 \quad (52)$$

We now substitute Ohm’s Law, which has no changing field strength, because of the homogeneity of the media:



$$j = \sigma E \quad (53)$$

(vectorial notation has been neglected because we work in 1D due to the actual geometrical symmetries). Hence:

$$\frac{\partial \rho}{\partial t} + \sigma \frac{\partial E}{\partial x} = 0 \quad (54)$$

On the other hand (Maxwell's Equation, Gauss Law):

$$\frac{\partial E}{\partial x} = \frac{\rho}{\varepsilon} \quad (55)$$

Substituting these into the continuity equation we obtain:

$$\frac{\partial \rho}{\partial t} = -\frac{\sigma}{\varepsilon} \rho \quad (56)$$

By solving this equation, we now have:

$$\rho = \rho_0 e^{-\frac{t}{\tau}}, \quad \tau = \frac{\varepsilon}{\sigma} \quad (57)$$

The space charge distortion now decays by the time constant:

$$\tau = \frac{\varepsilon}{\sigma} \quad (58)$$

If this time constant is larger than one-quarter of the periodic time of the supply, then we must calculate the space charge development in the homogeneous tissue as well.

Let us make an estimation for two tissues:

$$\begin{aligned} \varepsilon_{rfat} &= 30, & \sigma_{fat} &= 0.053 S/m \\ \varepsilon_{rmusc} &= 200, & \sigma &= 0.7 S/m \end{aligned} \quad (59)$$

Hence:

$$\begin{aligned} \tau_{fat} &= \frac{\varepsilon_0 \varepsilon_{rfat}}{\sigma_{fat}} \approx \frac{10^{-12} 30}{0.053 S/m} \approx 6 \cdot 10^{-10} s = 0.6 ns \\ \tau_{musc} &= \frac{\varepsilon_0 \varepsilon_{rmusc}}{\sigma_{musc}} \approx \frac{10^{-12} 200}{0.7 S/m} = 4 \cdot 10^{-10} s = 0.3 ns \end{aligned} \quad (60)$$

This is a quick relaxation-making current in a shorter time than one period of 13.56 MHz:

$$T = \frac{1}{f} = \frac{1}{13.56 \cdot 10^6} = 7.310^{-8} = 73 ns \quad (61)$$

This means that the boundaries have the complete action of the induced space charge by polarization to complete the appropriate current density, but the tissue interior for a long time average has to be regarded as neutral at the purely applied 13.56 MHz carrier frequency. The low-frequency modulation changes the situation. The charge separation at the boundaries introduces non-linearity, having a rectification effect that makes the low-frequency modulation active on the carrier in deeper tissues as well. Modulated electro-hyperthermia (mEHT; popular name nanothermia, trade name oncothermia) [63], uses time-fractal pattern modulation [64], which allows the effects in deeper regions as well. The applied power in mEHT is on average one order of magnitude lower than the power of other hyperthermia methods. The mEHT has an extreme selection (nano range [65]) and high SAR in transmembrane proteins of malignant cell-membrane [66]. This method produces massive apoptosis [67] and, in consequence of the created damage-associated molecular pattern [68], we expect systemic immune reactions (abscopal effect) as well [69, 70]. These effects ensure that positive clinical results [71] prove the concept of the moderate SAR and mild-temperature application [65].

## Conclusions

The internal polarization effects induce an injury current when any disturbance changes the healthy homeostatic equilibrium. An electric field in the direction of the place of disturbance from the healthy neighborhood appears, starting a current, which promotes cell migrations and wound healing, re-establishing homeostatic equilibrium. In pathological



disturbance, the same process starts, which supports further proliferation, so its blocking is desired. The ECT method is typical for this particular anti-injury current treatment, based on BCEC theory. However, its invasive way and special localization do not satisfy. We have shown that non-invasive external fields can produce a charge distribution in the macro and micro range, which can produce an anti-injury current.

## REFERENCES

- [1] Debye, P. 1913. *Ver. Deut. Phys. Gesell.* 15, 777; reprinted 1954 in collected papers of Peter J.W. Debye Interscience, New York.
- [2] Schwan, HP. 1963. Determination of biological impedances. In: *Physical Techniques in Biological Research*. Vol. 6, Academic Press, New York, pp. 323–406.
- [3] Schwan, HP., Takashima, S., Miyamoto, VK., and Stoeckenius, W. 1970. Electrical Properties of Phospholipid Vesicles; *Biophysical Journal* 10:1102–1119.
- [4] Leveen, H.H., Wapnick, S., Piccone, V., Falk, G., and Ahmed, N. 1976. Tumor eradication by radiofrequency therapy. *J. Amer. Med. Ass.* 235:2198–2200.
- [5] Martinsen, OG., Grimnes, S., and Schwan, HP. Interface Phenomena and Dielectric Properties Of Biological Tissue; *Encyclopedia of Surface and Colloid Science*, pp. 2643–2652.
- [6] Mafe, S., Pellicer, J., and Aguilera, VM. 1986. Ionic transport and space charge density in electrolytic solutions as described by Nernst-Planck and Poisson equations; *J. Phys. Chem.*, 90:6045–6050.
- [7] Schmuck, M., and Bazan, MZ. Homogenization of The Poisson-Nernst-Planck Equations For Ion Transport In Charged Porous Media; *SIAM J on Applied Mathematics*, 75(3).
- [8] Szasz, O., and Szasz, A. 2016. Heating, efficacy and dose of local hyperthermia. *Open Journal of Biophysics*, 6:10-18, <http://www.scirp.org/journal/PaperInformation.aspx?paperID=62874>.
- [9] LeVeen, H.H., Wapnick, S., Piccone, V., Falk, G., and Ahmed, N. 1976. Tumor eradication by radiofrequency therapy. *J. Amer. Med. Ass.* 235:2198–2200.
- [10] Szasz, A., Szasz, O., and Szasz, N. 2006. Physical background and technical realization of hyperthermia. In: Baronzio GF, Hager ED (eds) *Locoregional Radiofrequency-Perfusional- and Wholebody- Hyperthermia in Cancer Treatment: New clinical aspects*, Springer, New York, NY, pp. 27–59.
- [11] Bryant, DM., and Mostov, KE. 2008. From cells to organs: building polarized tissue. *Nat Rev Mol Cell Biol.* 9:887–901
- [12] Foulds, IS., and Barker, AT. 1983. Human skin battery potentials and their possible role in wound healing. *Br J Dermatol.* 109:515–522.
- [13] Cope, FW. 1969. Nuclear magnetic resonance evidence using D2O for structured water in muscle and brain. *Biophys J* 9:303–319.
- [14] Rosch, PJ., and Markov, MS. 2004. *Bioelectromagnetic medicine*. Marcell Decker Inc, New York.
- [15] Reid, B., McCaig, CD., and Zhao, M. et al 2005. Wound healing in rat cornea: the role of electric currents. *FASEB J* 19:379–386.
- [16] Barker, AT., Jaffe, LF., and Venable, JW Jr. 1982. The glabrous epidermis of cavies contains a powerful battery. *Am J Physiol* 242:R358–R366.
- [17] Samuelsson, L., Jonsson, L., and Stahl, E. 1983. Percutaneous treatment of pulmonary tumors by electrolysis. *Radiologie* 23:284–287.
- [18] Song, B., Zhao, M., and Forrester, J. et al 2004. Nerve regeneration and wound healing are stimulated and directed by an endogenous electrical field in vivo. *Journal of Cell Science* 117(20):4681–4690.
- [19] Carbon, M., Wübbeler, G., and Mackert, B-M. et al 2004. Non-invasive magnetic detection of human injury currents. *Clinical Neurophysiology* 115:1027–1032.
- [20] Reid, B., Nuccitelli, R., and Zhao, M. 2007. Non-invasive measurement of bioelectric currents with a vibrating probe. *Nature Protocols* 2:661–669.
- [21] Mackert, B-M., Mackert, J., and Wübbeler, G. et al 1999. Magnetometry of injury currents from human nerve and muscle specimens using superconducting quantum interferences devices. *Neuroscience Letters* 262:163–166.
- [22] Song, B., Zhao, M., and Forrester, JV. et al 2002. Electrical cues regulate the orientation and frequency of cell division and the rate of wound healing in vivo. *PNAS* 99:13577–13582.



- [23] Zhao, M. 2009. Electrical fields in wound healing—An overriding signal that directs cell migration. *Semin Cell Dev Biol* 20:674–682.
- [24] Huttenlocher, A. 2007. Wound healing with electric potential *NEJM*; 356:304–305.
- [25] Becker, RO., and Selden, G. 1985. *The body electric*. Morrow, New York.
- [26] Becker, RO., 1990. *Cross Currents*. Jeremy P Tarcher Inc., Los Angeles.
- [27] Kloth, LC., 2005. Electrical Stimulation for Wound Healing: A Review of Evidence From In Vitro Studies, Animal Experiments, and Clinical Trials; *Lower Extremity Wounds* 4:23–44.
- [28] Cheng, K., Tarjan, P., and Oliveira-Gandia, M. et al 1995. An occlusive dressing can sustain natural electrical potential of wounds. *J Invest Dermatol*;104:662–665.
- [29] Zhao, M., Song, B., and Pu, J. et al 2006. Electrical signals control wound healing through phosphatidylinositol-3-OH kinase- and PTEN. *Nature*, 442:457–460.
- [30] Zhao, M., Forrester, JV., and McCaig, CD. 1999. A small, physiological electric field orients cell division; *Proc. Natl. Acad. Sci. USA*; *Cell Biology* 96:4942–4946.
- [31] Zhao, M. 2009. Electrical fields in wound healing—An overriding signal that directs cell migration; *Seminars in Cell & Developmental Biology*, 20(6):674–682.
- [32] McCaig, C.D., Rajnicek, A.M., and Song, B. et. al. 2005. Controlling Cell Behaviour Electrically: Current Views and Future Potential. *Physiol. Rev.* 85:943–978.
- [33] Song, B., Zhao, M., Forrester, J., and McCaig, CD. 2004. Nerve regeneration and wound healing are stimulated and directed by an endogenous electrical field in vivo; *Journal of Cell Science* 117:4681–4690.
- [34] Mackert, B-M., Mackert, J., Wubbeler, G., Armbrust, F., Wolff, K-D., Burghoff, M., Trahms, L., and Curio, G. 1999. Magnetometry of injury currents from human nerve and muscle specimens using superconducting quantum interferences devices; *Neuroscience Letters* 262:163–166.
- [35] Carbon, M., Wbbeler, G., Mackert, B-M., Mackert, J., Ramsbacher, J., Trahms, L., and Curio, G. 2004. Non-invasive magnetic detection of human injury currents; *Clinical Neurophysiology* 115:1027–1032.
- [36] Reid, B., Nuccitelli, R., and Zhao, M. Non -invasive measurement of bioelectric currents with a vibrating probe 2007. *Nature Protocols* 3:661–670.
- [37] Becker, RO. Selden G 1985. *The body electric*. Morrow, New York.
- [38] Becker, RO. 1990. *Cross Currents*. Jeremy P Tarcher Inc., Los Angeles.
- [39] Nordenstrom, BWE. 1983. *Biologically Closed Electric Circuits: Clinical experimental and theoretical evidence for an additional circulatory system*. Nordic Medical Publications, Stockholm, Sweden.
- [40] Nordenstrom, BWE. 1998. *Exploring BCEC-systems, (Biologically Closed Electric Circuits)*. Nordic Medical Publications, Stockholm, Sweden.
- [41] James, AM., Ambrose, EJ., and Lowick JHB 1956. Differences between the electrical charge carried by normal and homologous tumor cells. *Nature* 177:576–577.
- [42] Binggeli, R., and Weinstein, RC. 1986. Membrane potentials and sodium channels: hypotheses for growth regulation and cancer formation based on changes in sodium channels and gap junctions. *J Theor Biol* 123:377–401.
- [43] Levin, M. 2007. Large-scale biophysics: ion flows and regeneration; *Trends in Cell Biology*, 17:261–270.
- [44] Mycielska, ME., and Djamgoz, MBA. 2004. Cellular mechanisms of direct-current electric field effects: galvanotaxis and metastatic disease. *J Cell Sci* 117:1631–1639.
- [45] Pu, J., McCaig, CD., and Cao, L. et al 2007. EGF receptor signalling is essential for electric-field-directed migration of breast cancer cells. *J Cell Sci* 120:3395–3403.
- [46] Meng, X., Riordan, NH. 2006. Cancer is a functional repair tissue. *Medical Hypotheses* 66:486–490.
- [47] Nordenström, BEW. 1978. Preliminary clinical trials of electrophoretic ionization in the treatment of malignant tumors. *IRCS Med Sci* 6:537.
- [48] Nordenström, BEW. 1985. Electrochemical treatment of cancer. *Ann Radiol* 28:128–129.



- [49] Sersa, G., Miklavcic, D., and Cemazar, M. et al 2008. Electrochemotherapy in treatment of tumors. *Eur J Surg Oncol* 34(2):232–240.
- [50] The first international conference on the topic was in Beijing, China, 20–22 October 1992. (200 Chinese and 30 foreign participants, one-hundred-thirty-six papers were presented), from that time in every second year regularly held, special international organization (IABC) organized with the center in USA.
- [51] Watson, BW. 1991. Reappraisal: The treatment of tumors with direct electric current. *Med Sci Res* 19:103–105.
- [52] Miklavcic, D., Sersa, G., and Kryzanowski, M. et al 1993. Tumor treatment by direct electric current, tumor temperature and pH, electrode materials and configuration. *Bioelectr Bioeng* 30:209–220.
- [53] Xin, Y-L. 1994. Organization and Spread electrochemical therapy (ECT) in China. *Eur J Surg S*, 574:25–30; Xin Y-L (1994) Advances in the treatment of malignant tumors by electrochemical therapy (ECT) *Eur J Surg S*, 574:31–36.
- [54] Matsushima, Y., Takahashi, E., and Hagiwara K et al 1994. Clinical and experimental studies of anti-tumoral effects of electrochemical therapy (ECT) alone or in combination with chemotherapy. *Eur J Surg S*, 574:59–67.
- [55] Chou, CK. et al 1999. Development of Electrochemical treatment at the City of Hope (USA). *Electricity and Magnetism in Biology and Medicine In: Bersani (ed) Kluwer Acad Press/Plenum Publ*, pp. 927–930.
- [56] Xin, Y., Xue, F., and Ge, B. et al 1997. Electrochemical treatment of lung cancer. *Bioelectromagnetics* 18:8–13.
- [57] Robertson, GS., Wemyss-Holden, SA., and Dennison, AR. et al 1998. Experimental study of electrolysis-induced hepatic necrosis. *British J Surgery* 85:1212–1216.
- [58] Jaroszeski, MJ., Coppola, D., and Pottinger, C. et al 2001. Treatment of hepatocellular carcinoma in a rat model, using electrochemotherapy. *Eur J Cancer* 37:422–430.
- [59] Holandino, C., Veiga, VF., and Rodriques, ML. et al 2001. Direct current decreases cell viability but not P-glycoprotein expression and function in human multidrug resistant leukemic cells. *Bioelectromagnetics* 22:470–478.
- [60] Susil, R., Semrov, D., and Miklavcic, D. 1998. Electric field-induced transmembrane potential depends on cell density and organization. *Electro- and Magnetobiology* 17:391–399.
- [61] Loewenstein, WR. 1999. *The touchstone of life, Molecular information, cell communication and the foundations of the life.* Oxford University Press, Oxford, New York, pp. 298–304.
- [62] Bard, AJ., and Faulkner, LR. 2000. *Electrochemical Methods, Fundamentals and Applications.* John Wiley & Sons Inc., New York.
- [63] Szasz, A., Szasz, N., and Szasz, O. 2010. *Oncothermia – Principles and practices.* Springer Science, Heidelberg.
- [64] Szasz, A. 2013. Electromagnetic effects in nanoscale range. *Cellular Response to Physical Stress and Therapeutic Applications* (eds. Tadamichi Shimizu, Takashi Kondo), chapter 4. Nova Science Publishers, Inc.
- [65] Vincze, Gy., Szigeti, Gy., Andocs, G., and Szasz, A. 2015. Nanoheating without Artificial Nanoparticles, *Biology and Medicine* 7(4):249.
- [66] Andocs, G., Rehman, MU., Zhao, QL., Papp, E., Kondo, T., and Szasz, A. 2015. Nanoheating without Artificial Nanoparticles Part II. Experimental support of the nanoheating concept of the modulated electro-hyperthermia method, using U937 cell suspension model, *Biology and Medicine* 7(4):1–9.
- [67] Meggyeshazi, N., Andocs, G., Balogh, L., Balla, P., Kiszner, G., Teleki, I., Jeney, A., and Krenacs, T. 2014. DNA fragmentation and caspase-independent programmed cell death by modulated electrohyperthermia. *Strahlenther Onkol* 190:815–822.
- [68] Andocs, G., Meggyeshazi, N., Balogh, L., Spisak, S., Maros, ME., Balla, P., Kiszner, G., Teleki, I., Kovago, Cs., and Krenacs, T. 2014. Upregulation of heat shock proteins and the promotion of damage-associated molecular pattern signals in a colorectal cancer model by modulated electrohyperthermia. *Cell Stress and Chaperones* 20(1):37–46.
- [69] Qin, W., Akutsu, Y., Andocs, G., Sugnami, A., Hu, X., Yusup, G., Komatsu-Akimoto, A., Hoshino, I., Hanari, N., Mori, M., Isozaki, Y., Akanuma, N., Tamura, Y., Matsubara, H. 2014. Modulated electro-hyperthermia enhances dendritic cell therapy through an abscopal effect in mice. *Oncol Rep*.
- [70] Tsang, Y., Huang C.C., Yang, K. L., Chi, M.S., Chiang, H.C., Wang, Y.S., Andocs, G., Szasz, A., Li W.T., Chi K. H. 2015. Improving immunological tumor microenvironment using electro-hyperthermia followed by dendritic cell immunotherapy, *BMC Cancer* 15:708.



---

[71] Szasz, A., Iluri, N., Szasz, O. 2013. Local hyperthermia in Oncology – To Choose or not to Choose? Hyperthermia, Ed: Huilgol N.



This work is licensed under a Creative Commons Attribution 4.0 International License.

DOI:10.24297/jab.v10i2.6328